Polym. Korea, Vol. 45, No. 6, pp. 841-848 (2021)
https://doi.org/10.7317/pk.2021.45.6.841

ISSN 0379-153X(Print)
ISSN 2234-8077(Online)

선택적 수용성 차수재 개발을 위한 나트륨-알지네이트/폴리아크릴아마이드 하이드로겔의 수용 속도 제어

최광묵† · 최진주 · 김우철* · 황환민** · 김명웅** · 김민준†

고등기술연구원 신소재공정센터, *한국지역난방공사 미래개발원, **인하대학교 화학·화학공학 융합학과

(2021년 3월 17일 접수, 2021년 5월 20일 수정, 2021년 6월 2일 채택)

Control of Dissolution Rate of Sodium-Alginate/Polyacrylamide Hydrogel for Selectively Dissolvable Water-Blocking Device

Gwang-Mook Choi†, Jin-Ju Choi, Woo-Cheol Kim*, Hwanmin Hwang, Myungwoong Kim**, and Min-Jun Kim†**

Advanced Materials & Processing Center, Institute for Advanced Engineering, Yongin 17180, Korea
**R & D Institute, Korea District Heating Corp., Yongin 17099, Korea*
***Department of Chemistry and Chemical Engineering, Inha University, Incheon 22212, Korea*

(Received March 17, 2021; Revised May 20, 2021; Accepted June 2, 2021)

초록: 본 연구에서는 나트륨-알지네이트/폴리아크릴아마이드(SA/PAM) 하이드로겔의 온도 및 가교제로 작용하는 *N,N′*-메틸렌비스아크릴아마이드(MBAAm) 농도에 따른 수용 형태 및 시간 변화를 분석하였다. 실험 결과, 수온이 증가하거나 가교제 농도가 감소할수록 SA/PAM 하이드로겔의 팽윤 및 수용 속도가 증가함을 확인하였다. 수온 상승 시 이온결합이 불안정하고 아마이드 결합이 깨지면서 하이드로겔의 수용 속도를 증가시키는 반면, MBAAm의 밀도 감소 시에는 주요 결합력인 이온결합력이 약화되어 고온수에 취약함을 확인하였다. 본 연구를 통해 SA/PAM 하이드로겔의 수용속도의 제어가 가능함을 증명하였고 선택적 수용이 가능한 차수재로서의 가능성을 제시하였다.

Abstract: The objective of this study was to examine changes in the dissolution rate of sodium-alginate/polyacrylamide (SA/PAM) hydrogel according to water temperature and concentration of cross-linking agent *N,N′*-methylenebisacrylamide (MBAAm). Results confirmed that swelling and dissolution rates of the SA/PAM hydrogel were increased when the temperature of the water was increased or the amount of MBAAm was decreased. When water temperature was increased, ionic crosslinks became unstable and amide bonds were broken due to hydrolysis, causing the hydrogel to rapidly dissolve in the hot water. Also, after the amount of MBAAm was decreased, ionic crosslinks became dominant and SA/PAM hydrogel became more vulnerable to hot water. Here, we analyzed the dissolution rate of hydrogel following temperature and MBAAm density changes. We also developed a selectively dissolvable water-blocking hydrogel that could be stable in cold water and become dissolved quickly in hot water.

Keywords: sodium-alginate/polyacrylamide hydrogel, dissolution rate, temperature effect, cross-linking density effect, selectively dissolvable water-blocking material.

Introduction

A hydrogel is a three-dimensional network of hydrophilic polymers having a moisture content of 90%. Because hydrogels consist of water with skin-like softness, they are safe for human body and easy to fabricate into complex shapes.

Hydrogels are regarded as promising bio-compatible materials in various fields such as strain sensors,[1-4] wastewater absorbents,[5-8] and ultrasound imaging for diagnosis.[9-12] In the agricultural field, the high moisture content and porous structure of hydrogels enable them to be stored and to supply moisture in landfills. It has also been proven that crop productivity can be improved by storing necessary nutrients inside a hydrogel and continuously releasing them for a certain period of time.[13-15] In the medical field, the physicochemical similarity of hydrogels to human tissue has led to their application as scaffolds for tis-

†To whom correspondence should be addressed.
gmchoi@iae.re.kr, ORCID 0000-0002-1701-4578
minjun@iae.re.kr, ORCID 0000-0002-3339-1787

sue engineering,[16,17] cell culture,[18,19] and drug carriers.[20,21]

Despite these advantages, the weak mechanical properties of hydrogels have been major constraints. The fracture energy of hydrogel, such as a polyacrylamide hydrogel, is approximately 10 $J \cdot m^{-2}$, which is 1/1000 of that of natural rubber (10000 $J \cdot m^{-2}$). Fortunately, recent development of a sodium-alginate/polyacrylamide (SA/PAM) hydrogel has significantly improved mechanical properties of hydrogels. In 2012, SA/PAM hydrogel synthesized by adding sodium-alginate to polyacrylamide hydrogel was reported for the first time.[12] An alginate chain has guluronic acid blocks forming ionic crosslinks through ions, thus enhancing mechanical properties and resilience of the gel. The fracture energy of SA/PAM hydrogel is 9000 $J \cdot m^{-2}$, which is 900 times larger than that of normal hydrogels and similar to that of natural rubber.[22]

In this study, we determined the dissolution rate of SA/PAM hydrogel in water. Our results confirmed that the dissolution rate of SA/PAM hydrogels could be controlled by adjusting water temperature and cross-linker concentration. Ionic cross-links between ions and alginate play a significant role in mechanical properties of SA/PAM hydrogels. When water temperature was increased and cross-linking agent concentration was decreased, the stability of ionic crosslinks was reduced, which broke them down and dissolved the hydrogel quickly. Amide bonds were also broken since hydrolysis became dominant rather than recombination reaction according to temperature and cross-linker concentration. Therefore, the dissolution rate varied depending on the water temperature and the concentration of the cross-linking agent.

Due to their excellent mechanical properties and dissolution rate control, SA/PAM hydrogels are suitable water-blocking materials for repairing pipes. The interior of an actual pipe is rough and uneven owing to oxidation and corrosion. With conventional water-blocking methods such as rubber-balloon method are used for pipes, such irregularities cannot be covered. Hence, the working environment becomes increasingly unstable because of water leakage. On the other hand, soft properties of hydrogels are sufficient to fill in surface irregularities, thus preventing water leakage. Because SA/PAM hydrogels are biocompatible,[23] they are suitable as water-blocking materials for repairing or replacing pipes that transport water in our daily life. Finally, because dissolution rate can be controlled by adjusting water temperature and cross-linking agent concentration, SA/PAM hydrogel-based water-blocking devices can be easily removed without the process of taking them out by supplying hot water into the pipe after a repair or replacement, making them very convenient and efficient.

The SA/PAM hydrogel production conditions that provide the highest mechanical strength were selected by analyzing mechanical properties and microstructures of SA/PAM hydrogels according to the concentration of the cross-linking agent, *N,N′*-methylenebisacrylamide (MBAAm). Dissolution rate of the SA/PAM hydrogel was then analyzed according to water temperature and cross-linking agent concentration by examining the shape, swelling ratio, and Na^+ concentration in water at each hour and the dissolution time. After manufacturing an optimal SA/PAM hydrogel water-blocking device based on results obtained, whether it could be used as an actual water-blocking material was determined by measuring water-proof time for each water temperature through a pipe model similar to the actual pipeline construction environment.

Experimental

Synthesis of SA/PAM Hydrogel. SA/PAM hydrogels were synthesized with the following method. First, an acrylamide (DUKSAN, Korea) 50 wt% aqueous solution was prepared and stirred at room temperature for 24 h. Then 4.5 g of $NaHCO_3$ (DUKSAN, Korea) was added to a sodium-alginate (Sigma-aldrich, USA) 2 wt% aqueous solution and stirred at room temperature for 48 h. If $NaHCO_3$ was added immediately during the experiment, then the dissolution rate was low and the solution was not uniformly mixed. To make a cross-linker solution, a 1 wt% MBAAm (Sigma-aldrich, USA) aqueous solution was prepared and stirred at room temperature for 24 h and a 10 wt% aqueous ammonium persulfate (APS, Sigma-aldrich, USA) solution was prepared to make an initiator solution. Finally, a 10 wt% tetramethylethylenediamine (TEMED, Sigma-aldrich, USA) aqueous solution was prepared and stirred at room temperature for 24 h to make an accelerator solution.

These prepared solutions were weighed and mixed as follows. First, 12.44 g of 50 wt% acrylamide aqueous solution was added to 39.6 g of a mixed aqueous solution of sodium alginate and $NaHCO_3$. Then, 0.4 g of 1 wt% TEMED aqueous solution and 1 wt% MBAAm were mixed and dissolved. The amount of MBAAm added was adjusted to 0.1, 0.2, 0.3, 0.4, and 0.5 g to prepare hydrogels with different concentrations of the cross-linking agent. Finally, after adding 0.62 g of 10 wt% APS aqueous solution, the mixed solution was placed in a mold, stirred using a glass rod, and heated in a 40 °C oven for

20 h. The mold was placed in a sealed container to prevent moisture loss.

Tensile Strength and Microstructure Analysis. The tensile strength of the hydrogel was analyzed using a universal testing machine (Yeonjin S-Tech, Korea) with a maximum load of 100 kg (1 kN). Hydrogel tensile specimens were prepared at size of 5 mm (Width)×5 mm (Height)×40 mm (Length). The initially analyzed length was set to be 20 mm by fixing each 10 mm up and down using a jig during the tensile test. The tensile speed was set at 10 mm/min until failure occurred. With regard to the hydrogel microstructure, hydrogel specimens with different MBAAm contents were frozen at 20 °C for 48 h, and then placed in a freeze dryer for 24 h. The microstructure of the cross-section according to the MBAAm content was determined using a field-emission scanning electron microscopy (FE-SEM, TESCAN, Korea).

Dissolution Rate Analysis According to Water Temperature and MBAAm Content. To confirm the effect of MBAAm content on dissolution rate, hydrogels with various MBAAm contents of 0.1, 0.2, 0.3, 0.4, and 0.5 g were analyzed at 100 °C. First, 400 mL of distilled water was heated to boiling. An autoclave container capable of maintaining a constant pressure and temperature was filled with boiling water. Then a 20 mm×20 mm×10 mm hydrogel specimen was placed in the autoclave container. Its weight, size, and shape were analyzed every hour to confirm swelling and dissolution. For accurate analysis, the size and weight were measured after removing water on the surface. The swelling ratio was calculated using the following eq.:

$$\text{Swelling ratio (\%)} = \frac{(\text{Weight after swelling} - \text{Initial weight})}{\text{Initial weight}} \times 100 \quad (1)$$

In the case of dissolution rate according to temperature, water-soluble state was analyzed at 80, 90, 100, 110, and 120 °C using a hydrogel containing 0.4 g of MBAAm, which had the highest mechanical strength.

Also, to confirm ionic bond breaking between alginate and sodium ions, concentrations of sodium ions were analyzed through inductively coupled plasma-atomic emission spectrometry (ICP-AES, Agilent tech, USA) analysis of the aqueous solution in which hydrogels were dipped.

Results and Discussion

Mechanical Strength and Microstructure of Hydrogel According to MBAAm Content. Figure 1 shows tensile test results of the SA/PAM hydrogel according to the MBAAm content. When the MBAAm content was below 0.4 g, elastic modulus and tensile strength were increased with increasing MBAAm content. When the MBAAm content was 0.5 g, the elastic modulus of the hydrogel was increased but the toughness was decreased due to a decrease of elongation. These results showed that the network cross-linking density was gradually increased with increasing MBAAm content and elastic modulus of the hydrogel. However, as the hydrogel rigidity increased with excessive addition of MBAAm, the elastic modulus was increased, but the elongation was decreased.

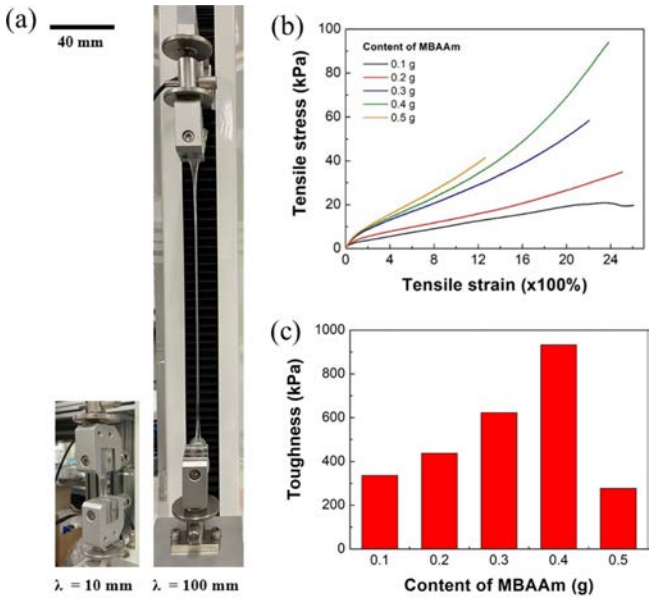

Figure 1. Tensile test of SA/PAM hydrogel: (a) image of measuring tensile stress of hydrogel (λ: distance between the two clamps); (b) tensile stress-strain curve of hydrogels according to the content of crosslinker, MBAAm; (c) toughness of hydrogels according to the content of MBAAm.

Figure 2 shows microstructures of SA/PAM hydrogels according to the MBAAm content using FE-SEM. Results showed that the larger the MBAAm content, the smaller the pore size. This means that the MBAAm can make the hydrogel dense by connecting between polyacrylamides.[23] In addition, because the increase in the elastic modulus with the increase in MBAAm content improved the expansion resistance, the expansion effect of swelling was relatively small. Thus, the pore size appeared relatively small.

Dissolution Rate According to Water Temperature. Figures 3 and 4 show experimental results of the dissolution rate of SA/PAM hydrogel according to water temperature. Results

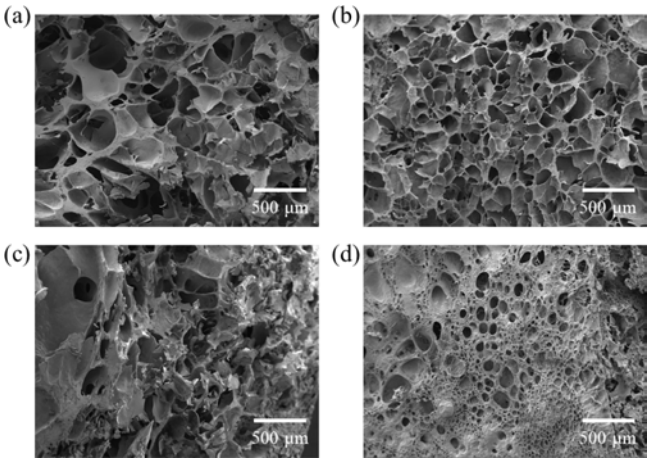

Figure 2. Microstructures of SA/PAM hydrogels according to MBAAm content: (a) 0.1 g; (b) 0.2 g; (c) 0.3 g; (d) 0.4 g.

confirmed that the swelling ratio was increased more rapidly as water temperature increased. However, at 120 °C, the swelling ratio rapidly decreased after 2 h. Specifically, the swelling ratio of SA/PAM hydrogels increased from 987 to 2288% at 80 °C, from 1410 to 2438% at 90 °C, and from 1521 to 2783% at 100 °C after exposure for 1 to 5 h. Results confirmed that the higher the temperature, the faster the initial swelling rate. However, the swelling rate gradually decreased over time. Results of specimen observations confirmed that the original shape of the specimen was maintained at ≤100 °C. This meant that the cross-linking reaction in the water-soluble composite polymer was resistant to hot water up to 100 °C. At 110 °C, the swelling ratio increased from 1936 to 3612% as the swelling time increased from 1 to 5 h. Despite swelling, the original shape of the specimen was maintained for 1 h. However, after 3 h, the SA/PAM hydrogel was liquefied, indicating that cross-linking in the hydrogel gradually weakened. When the swelling time of the hydrogel was increased from 1 h to 2 h at 120 °C, the swelling ratio increased from 2144 to 3066%, but decreased to 993% after 3 h and completely dissolved after 4 h.

This tendency was originated from the breaking of ionic bonding between alginate and sodium ions and the hydrolysis of polyacrylamide. First, the ionic bonding between alginate and sodium ions was weakened. The higher the water temperature, the more easily ions could form the ionic bond with the alginate in hydrogel escape, thus weakening the ionic bonding force and consequently dissolving the hydrogel. To confirm this, the sodium concentration of water in which the hydrogel was dipped for 1 h was analyzed by ICP-AES (Figure 4(b)). Results showed that at 80, 90, 100, 110 °C, and 120

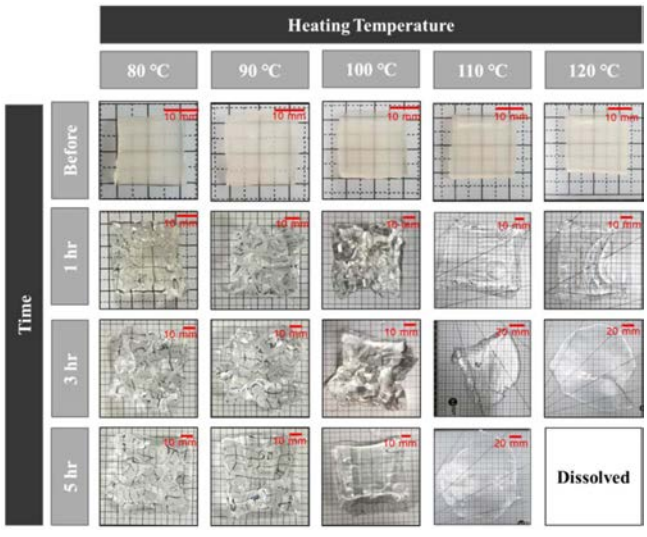

Figure 3. Shape of SA/PAM hydrogel with 0.4 g MBAAm according to swelling time and temperature of the water in which hydrogels were dipped. The size of each sample before test was 20 mm (width)×20 mm (length)×5 mm (height).

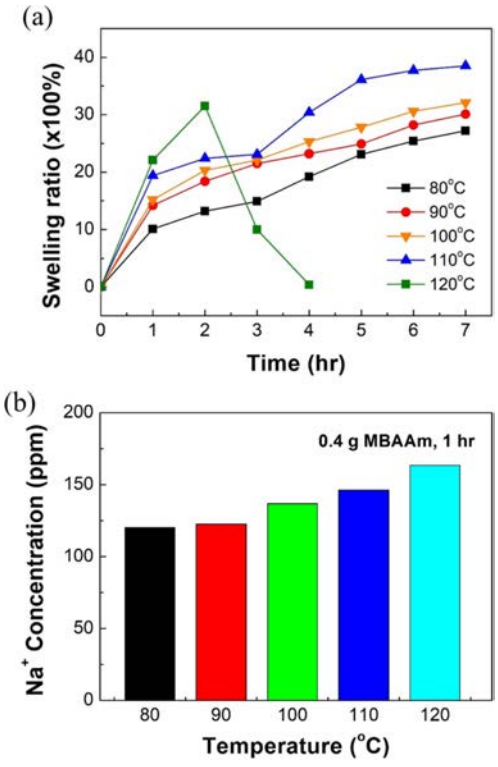

Figure 4. Swelling tendency of SA/PAM hydrogel with 0.4 g MBAAm according to temperature of the water in which hydrogels were dipped: (a) swelling ratio of SA/PAM hydrogel over swelling time; (b) Na^+ concentrations of water in which hydrogels were dipped.

°C, sodium concentrations were 120.27, 122.55, 136.81, 146.22, and 163.38 ppm, respectively, indicating that the higher the actual temperature, the greater the number of sodium ions that would escape. Second, amide bonding was broken due to hydrolysis. According to existing studies,[24-27] polyamide generally tends to reach the molecular weight that achieves dynamic equilibrium through competition between hydrolysis and recombination reaction. When polyamide with a high molecular weight is exposed to a high temperature and/or a high pressure, hydrolysis takes place more actively than recombination reaction. Thus, amide bonds will break and polyamide will melt. Therefore, it seems that the higher the temperature, the faster the dissolution rate as ionic and amide bonds are broken.

Dissolution Rate According to the Content of MBAAm.

Figures 5 and 6 show swelling ratios of SA/PAM hydrogels with different MBAAm contents after placing them in 100 °C water. In the case of the hydrogel with 0.1 g MBAAm, the swelling ratio increased during the first hour. It then decreased from 2 h onward. It was fully dissolved in approximately 3 h. In the case of the hydrogel with 0.2 g MBAAm, the swelling ratio increased for 3 h. It then began to decrease after 4 h. It was completely dissolved after 7 h. In the case of the hydrogel with 0.3 g MBAAm, the swelling ratio increased during the initial 5 h. It then decreased after 6 h. The swelling ratio of the hydrogel with 0.4 g MBAAm continuously increased. However, regardless of the MBAAm content, the rate of swelling ratio tended to decrease over time.

In the case of the 0.1 g MBAAm hydrogel, the dissolution rate was very high compared with the swelling rate. The swelling ratio seemed to decrease after 1 h of the experiment. In the case of the hydrogel with 0.2 g MBAAm, the swelling ratio was increased faster than that of hydrogel with 0.3 g or 0.4 g MBAAm because the lower the MBAAm content, the lower the swelling resistance, and the faster the swelling rate. As discussed above, the lower the MBAAm content, the larger the proportion of pores in the hydrogel, meaning that there were a lot of spaces to be filled with water inside the gel. In addition, the rigidity of the hydrogel was reduced and the swelling resistance decreased because expansion easily occurred. However, the hydrogel containing 0.2 g MBAAm also began to lose weight after 4 h, which might be because the swelling rate gradually decreased as the swelling gradually became saturated, while the dissolution rate was maintained. The hydrogel with 0.3 g MBAAm also showed a tendency to lose weight after 6 h of the experiment as the dissolution rate exceeded the swelling rate. However, in the case of the hydrogel with 0.4 g MBAAm, the rate of increase of the swelling ratio gradually

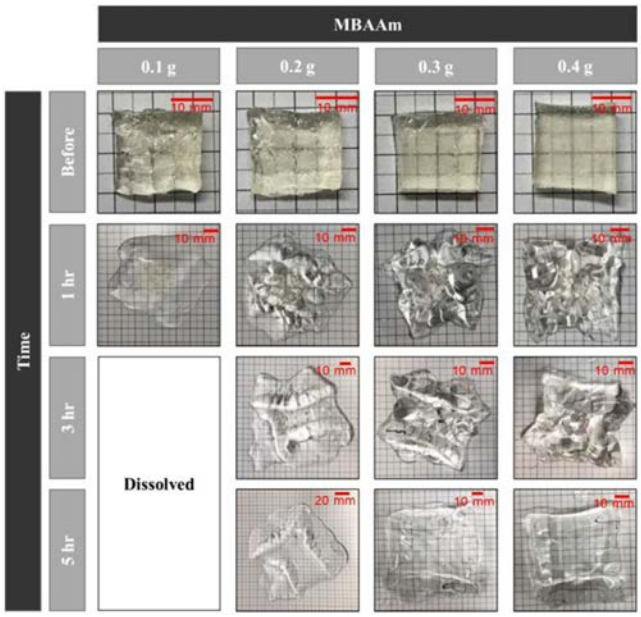

Figure 5. Shape of SA/PAM hydrogel in 100 °C water according to swelling time and MBAAm content. The size of each sample before test was 20 mm (width)×20 mm (length)×5 mm (height).

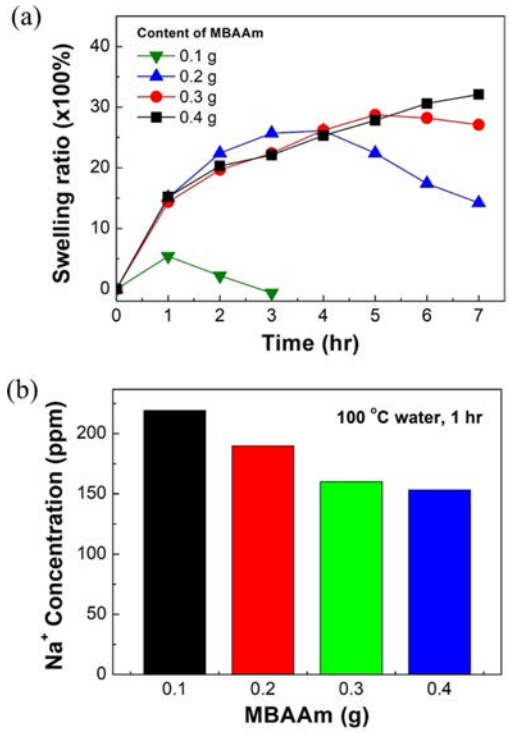

Figure 6. Swelling tendency of SA/PAM hydrogel according to MBAAm content in 100 °C water: (a) swelling ratio of SA/PAM hydrogel over swelling time; (b) Na^+ concentrations of water in which hydrogels were dipped.

decreased. However, it did not show a decrease. Thus, as the MBAAm concentration increased, the swelling resistance increased and the dissolution rate decreased. Hence, the swelling ratio appeared to increase for a longer period of time. These results confirmed that swelling and dissolution rates could be controlled by adjusting the concentration of MBAAm.

This tendency was attributed to the portion between ionic bonds and covalent bonds inside the hydrogel. As the MBAAm content decreased, the ionic bonding between sodium ions and alginate was relatively dominant among bonds, which maintained the shape of the hydrogel. When placed in hot water, the hydrogel with a low MBAAm content lost its shape and dissolved faster because sodium ions that retained the bond could easily escape. On the other hand, the higher the MBAAm content, the more the covalent bond with MBAAm became relatively dominant. The dissolution resistance of the hydrogel increased because covalent bonds could not be easily broken, even in hot water.

ICP-AES analysis was performed to confirm that sodium ions escaped differently according to the MBAAm content. Figure 6(b) shows sodium concentration of an aqueous solution in which hydrogels with different MBAAm contents were immersed in 100 °C water for 1 h. As the sodium concentration of the aqueous solution increased, concentrations of sodium ions inside the hydrogel decreased, indicating that the binding force between the ions and alginate was weakened. Analysis results showed that when MBAAm contents were 0.1, 0.2, 0.3, and 0.4 g, sodium concentrations were 175.24, 151.83, 128.12, and 122.55 ppm, respectively. These results confirmed that the sodium ion concentration of the aqueous solution decreased as the MBAAm content increased.

Water-Blocking Test of SA/PAM Hydrogel. To determine whether the SA/PAM hydrogel could be used as an actual water-blocking material in pipes, an optimal water-blocking material was manufactured based on its mechanical properties and dissolution rate. A balloon type water-blocking system was chosen because it was easy to insert it into the pipe to fill in the rough surface through expansion. Figure 7 shows the

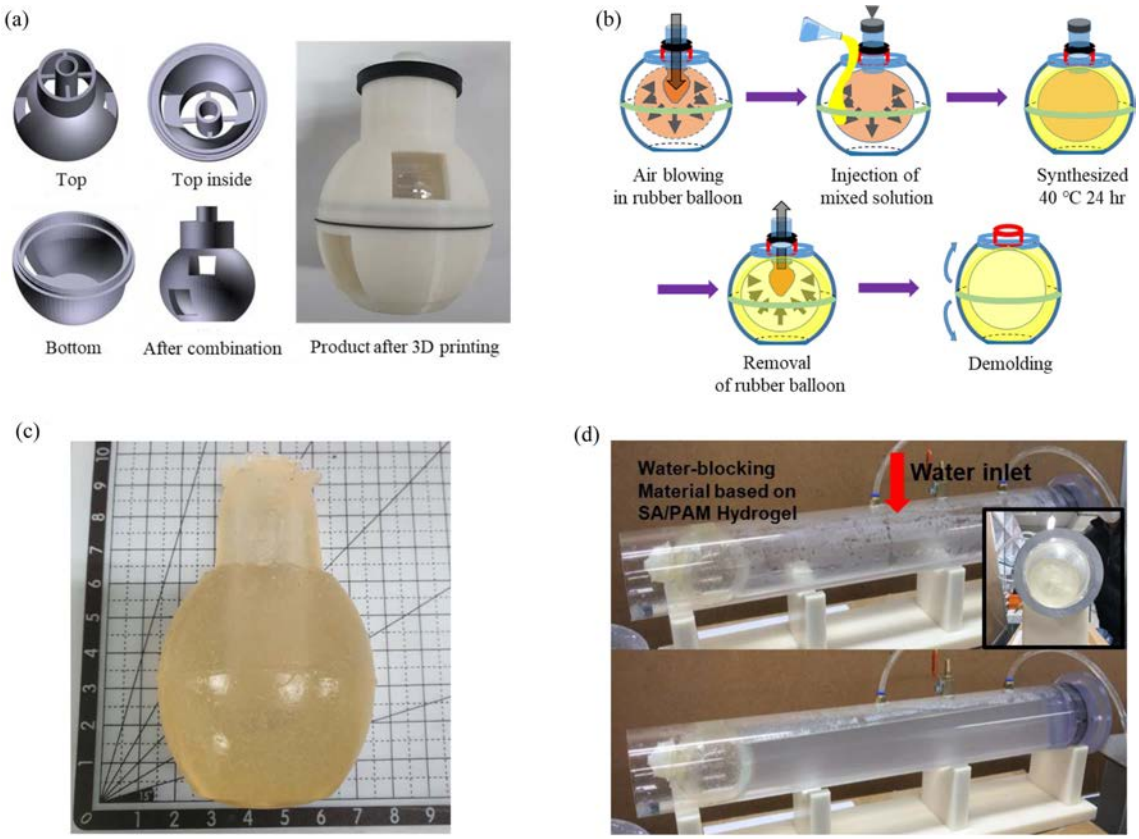

Figure 7. Water-blocking test of SA/PAM hydrogel in the pipe: (a) balloon-type mold made of ABS was fabricated by 3D printing; (b) manufacturing process of the balloon-type water-blocking material using the 3D printed mold; (c) water-blocking balloon made of SA/PAM hydrogel; (d) water-blocking test in a simulated pipe. Water was allowed to circulate inside the pipe to keep the water temperature constant.

process of manufacturing and testing the water-blocking balloon. The hydrogel with 0.4 g MBAAm, which had excellent mechanical properties, was adopted as the water-blocking material. To produce a balloon-shaped water-blocking material, a spherical-shaped mold made of polylactic acid was fabricated by 3D printing, and an inlet for injection was made at the top. At the center of the inlet, an insertion port capable of supporting a tube connected to a rubber balloon was made. After inserting the tube, air was blown into it to produce an empty balloon-shaped mold. Then, the mixed solution was injected into the prepared mold in the order of hydrogel production and heated at 40 °C for 24 h to synthesize a balloon-type hydrogel. After the synthesis, the inside of the balloon was deflated, the tube was removed, and upper and lower parts of the mold were separated to demold the hydrogel.

After inserting the manufactured balloon-type water-blocking material into the pipe, which had an inlet and an outlet for water circulation, air was blown in to block the pipe, and the hydrogel was sealed using a water-soluble PVA cable tie. Then the water heated in the heating bath was allowed to circulate inside the pipe to maintain a constant water temperature. The water-blocking time was measured at water temperatures of 25, 60, 70, and 80 °C.

Experimental results showed that the SA/PAM hydrogel-based balloon exploded after 310 min at 25 °C, 132 min at 60 °C, 35 min at 70 °C, and 20 min at 80 °C. These results confirmed that the higher the water temperature, the lower the water-blocking performance. The reason why the hydrogel exploded sooner than the previously analyzed dissolution time might be because it swelled under continuous tension after air injection. Through this experiment, it was confirmed that the SA/PAM hydrogel could effectively prevent water leakage when it was used to repair pipes. After the repair, it could be removed using hot water without an additional removal process.

Conclusions

In this study, the dissolution rate of the SA/PAM hydrogel was analyzed according to the temperature of water and the concentration of MBAAm. Results showed that the higher the MBAAm concentration, the slower the swelling rate in the water at the same temperature.

The swelling ratio of hydrogel was increased rapidly with an increasing temperature. However, the swelling ratio rapidly decreased after 2 h at temperature above 120 °C. This means that sodium ions in the hydrogel escaped easily at a high temperature and the hydrogel dissolved in water quickly. Also, amide bonds were broken since hydrolysis became dominant rather than a recombination reaction, which accelerated the dissolution rate. Results of ICP-AES analysis confirmed that concentrations of sodium ions that escaped from the hydrogel increased as the temperature increased.

Results of analysis of change in swelling ratio according to MBAAm concentration confirmed that the higher the MBAAm concentration, the slower the occurrence of swelling in water at the same temperature. This was attributed to an increase in swelling resistance as the MBAAm concentration increased. However, in the case of the hydrogel with 0.1 g MBAAm, the swelling ratio increased the slowest because the increase in the swelling rate was cancelled by the increase of the dissolution rate. The SA/PAM hydrogel maintained its shape through chemical bonding by MBAAm and ionic bonding by alginate and sodium ions. When swelling in hot water, the ionic bond between alginate and sodium ions was easily broken as ions inside the hydrogel escaped. Therefore, the lower the MBAAm content, the more dominant the ionic bonding force and the faster the dissolution rate. Results of ICP-AES analysis confirmed that the concentration of sodium ions coming out of the hydrogel increased at a lower MBAAm content.

These results confirmed that SA/PAM hydrogel could be used as a water-blocking balloon for repairing heating pipe without needing a separate removal process. To determine whether effective water blocking was possible, a pipe with a diameter of 80 mm, which simulated a real pipe, was fabricated and an experiment was conducted under conditions similar to the real environment. Results confirmed that the SA/PAM hydrogel-based balloon could resist swelling for 310 min at 25 °C and 132 min at 60 °C, providing sufficient time to repair the pipe. Thus, such SA/PAM water-blocking material can be used to repair metallic pipes (such as copper pipes, steel pipes, and stainless steel pipes known to be able withstand high temperatures), household drainage pipes, and heat transport pipe used for urban heating.

References

1. Guo, J.; Liu, X.; Jiang, N.; Yetisen, A. K.; Yuk, H.; Yang, C.; Khademhosseini, A.; Zhao, X.; Yun, S.-H. Highly Stretchable, Strain Sensing Hydrogel Optical Fibers. *Adv. Mater.* **2016**, 28, 10244-10249.
2. Liu, S.; Li, L. Ultrastretchable and Self-Healing Double-Network

Hydrogel for 3D Printing and Strain Sensor. *ACS Appl. Mater. Interfaces* **2017**, 9, 26429-26437.
3. Cai, G.; Wang, J.; Qian, K.; Chen, J.; Li, S.; Lee, P. S. Extremely Stretchable Strain Sensors Based on Conductive Self-Healing Dynamic Cross-Links Hydrogels for Human-Motion Detection. *Adv. Sci.* **2017**, 4, 1600190.
4. Xia, S.; Song, S.; Jia, F.; Gao, G. A Flexible, Adhesive and Self-Healable Hydrogel-Based Wearable Strain Sensor for Human Motion and Physiological Signal Monitoring. *J. Mater. Chem. B.* **2019**, 7, 4638-4648.
5. Yue, Y.; Wang, X.; Wu, Q.; Han, J.; Jiang, J. Assembly of Polyacrylamide-Sodium Alginate-Based Organic-Inorganic Hydrogel with Mechanical and Adsorption Properties. *Polymers* **2019**, 11, 1239.
6. Guo, H.; Jiao, T.; Zhang, Q.; Guo, W.; Peng, Q.; Yan, X. Preparation of Graphene Oxide-Based Hydrogels as Efficient Dye Adsorbents for Wastewater Treatment. *Nanoscale Res. Lett.* **2015**, 10, 272.
7. Pakdel, P. M.; Peighambardoust, S. J. A Review on Acrylic Based Hydrogels and Their Applications in Wastewater Treatment. *J. Environ. Manage.* **2018**, 217, 123-143.
8. Xiaofeng Yi, X.; Zhiqun Xu, Z.; Yan Liu, Y.; Xueyong Guo, X.; Minrui Ou, M.; Xiaoping Xu, X. Highly Efficient Removal of Uranium(VI) from Wastewater by Polyacrylic Acid Hydrogels. *RSC Adv.* **2017**, 7, 6278-6287.
9. Yi, J.; Nguyen, K. -C. T.; Wang, W.; Yang, W.; Pan, M.; Lou, E.; Major, P. W.; Le, L. H.; Zeng, H. Polyacrylamide/Alginate Double-Network Tough Hydrogels for Intraoral Ultrasound Imaging. *J. Colloid Interface Sci.* **2020**, 578, 598-607.
10. Ruland, A.; Gilmore, K. J.; Daikuara, L. Y.; Fay, C. D.; Yue, Z.; Wallace, G. G. Quantitative Ultrasound Imaging of Cell-Laden Hydrogels and Printed Constructs. *Acta Biomater.* **2019**, 91, 173-185.
11. Jiang, H.; Carter, N. M.; Zareei, A.; Nejati, S.; Waimin, J. F.; Chittiboyina, S.; Niedert, E. E.; Soleimani, T.; Lelièvre, S. A.; Goergen, C. J.; Rahimi, R. A Wireless Implantable Strain Sensing Scheme Using Ultrasound Imaging of Highly Stretchable Zinc Oxide/Poly Dimethylacrylamide Nanocomposite Hydrogel. *ACS Appl. Bio Mater.* **2020**, 3, 4012-4024.
12. Jiang, H.; Carrillo, K. T.; Kobayashi, T. Ultrasound Stimulated Release of Mimosa Medicine from Cellulose Hydrogel Matrix, Ultrason. *Sonochem*. **2016**, 32, 398-406.
13. Neethu, T. M.; Dubey, P. K.; Kaswala, A. R. Prospects and Applications of Hydrogel Technology in Agriculture. *Int. J. Curr. Microbiol. App. Sci.* **2018**, 7, 3155-3162.
14. El-Asmar, J.; Jaafar, H.; Bashour, I.; Farran, M. T.; Saoud, I. P. Hydrogel Banding Improves Plant Growth, Survival, and Water Use Efficiency in Two Calcareous Soils. *Clean-Soil Air Water* **2017**, 45, 1700251.
15. Saha, A.; Rattan, B.; Sekharan, S.; Manna, U. Quantifying the Interactive Effect of Water Absorbing Polymer (WAP)-Soil Texture on Plant Available Water Content and Irrigation Frequency. *Geoderma* **2020**, 368, 114310.
16. Zhu, J.; Hu, J.; Marchant, R. E. Biomimetic Scaffolds for Stem Cell Based Tissue Engineering. In *Biomimetic Biomaterials*, Ruys, A. Ed.; Woodhead Publishing: Sawston, 2013; pp 238-275.
17. Xiong, G.; Luo, H.; Gu, F.; Zhang, J.; Hu, D.; Wan, Y. A Novel *In Vitro* Three-Dimensional Macroporous Scaffolds from Bacterial Cellulose for Culture of Breast Cancer Cells. *J. Biomater. Nanobiotechnol.* **2013**, 4, 316-326.
18. McKinnon, D. D.; Kloxin, A. M.; Anseth, K. S. Synthetic Hydrogel Platform for Three-dimensional Culture of Embryonic Stem Cell-derived Motor Neurons. *Biomater. Sci.* **2013**, 1, 460-469.
19. Rustad, K. C.; Wong, V. W.; Sorkin, M.; Glotzbach, J. P.; Major, M. R.; Rajadas, J.; Longaker, M. T.; Gurtner, G. C. Enhancement of Mesenchymal Stem Cell Angiogenic Capacity and Stemness by a Biomimetic Hydrogel Scaffold. *Biomaterials* **2012**, 33, 80-90.
20. Serban, B. A.; Barrett-Catton, E.; Serban, M. A. Tetraethyl Orthosilicate-Based Hydrogels for Drug Delivery–Effects of Their Nanoparticulate Structure on Release Properties. *Gels* **2020**, 6, 38.
21. Zuckerman, S. T.; Rivera-Delgado, E.; Haley, R. M.; Korley, J. N.; von Recum, H. A. Elucidating the Structure-Function Relationship of Solvent and Cross-Linker on Affinity-Based Release from Cyclodextrin Hydrogels. *Gels* **2020**, 6, 9.
22. Sun, J.-Y.; Zhao, X.; Illeperuma, W. R. K.; Chaudhuri, O.; Oh, K. H.; Mooney, D. J.; Vlassak, J. J.; Suo, Z. Highly Stretchable and Tough Hydrogels. *Nature* **2012**, 489, 133-136.
23. Darnell, M. C.; Sun, J.-Y.; Mehta, M.; Johnson, C.; Arany, P. R.; Suo, Z.; Mooney, D. J. Performance and Biocompatibility of Extremely Tough Alginate/Polyacrylamide Hydrogels. *Biomaterials* **2013**, 34, 8042-8048.
24. Chavda, H. V.; Patel, C. N. Effect of Crosslinker Concentration on Characteristics of Superporous Hydrogel. *Int. J. Pharm. Investig.* **2011**, 1, 17-21.
25. Meyer, A.; Jones, N.; Lin, Y.; Kranbuehl, D. Characterizing and Modeling the Hydrolysis of Polyamide-11 in a pH 7 Water Environment. *Macromolecules* **2002**, 35, 2784-2798.
26. Matsushima, K.; Minoshima, H.; Kawanami, H.; Ikushima, Y.; Nishizawa, M.; Kawamukai, A.; Hara, K. Decomposition Reaction of Alginic Acid Using Subcritical and Supercritical Water. *Ind. Eng. Chem. Res.* **2005**, 44, 9626-9630.
27. Smith, R. M.; Hansen, D. E. The pH-Rate Profile for the Hydrolysis of a Peptide Bond. *J. Am. Chem. Soc.* **1998**, 120, 8910-8913.